Sterile neutrino signatures with Suzaku/朱雀

Maeda Yoshitomo
前田 良知 (ISAS/JAXA)

朱雀 is one of the four symbols of the Chinese constellations.

Provided by T. Tamura

An invited talk

In Astroparticle View of Galaxy Clusters,

2015 March in Hiroshima University

X-ray Hunt for Dark Matter in Clusters with Suzaku and ASTRO-H

Tamura Takayuki

In collaboration with Mitsuda,K., Yamasaki,N., Iizuka,R., Maeda,Y., Kamada,A., Yoshida,N., Kitayama, T.

Thanks to Matsushita,K., Boyarsky,A., Ruchayskiy, O., Bulbul,E. Takahashi,T., Sekiya, N.

List of Suzaku Results on X-ray Hunt for Dark Matter

- **Loewenstein, M., Kusenko, A., & Biermann, P. L. (2009) ApJ**
  "New Limits on Sterile Neutrinos from Suzaku Observations of the Ursa Minor Dwarf Spheroidal Galaxy"
- **Kusenko, A., Loewenstein, M., & Yanagida, T. (2013) Physical Review D**
  "Moduli dark matter and the search for its decay line using Suzaku X-ray telescope"
- **Tamura, T., Iizuka, R., Maeda, Y., Mitsuda, K. & Yamasaki, Y. N. (2015) PASJ**
  "An X-ray spectroscopic search for dark matter in the Perseus cluster with Suzaku"
- **Sekiya, N., Yamasaki, Y. N. & Mitsuda, K. (2015) arXiv:1504.02826**
  "A Search for a keV Signature of Radiatively Decaying Dark Matter with Suzaku XIS Observations of the X-ray Diffuse Background"

+ unpublished results

If you know more, please let us know.

(1) Introduction: X-ray search for dark matter, Sterile Neutrino, model and past observations

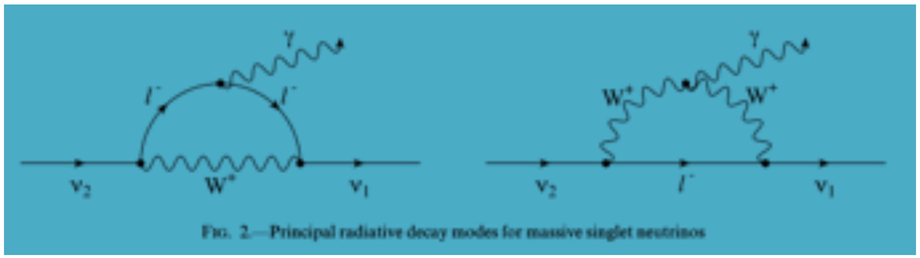

FIG. 2—Principal radiative decay modes for massive singlet neutrinos

By A. Foster

(3) *ASTRO-H* Observatory

To be launched in 2015…

(2) *Suzaku* X-ray search for unidentified lines

Currently…

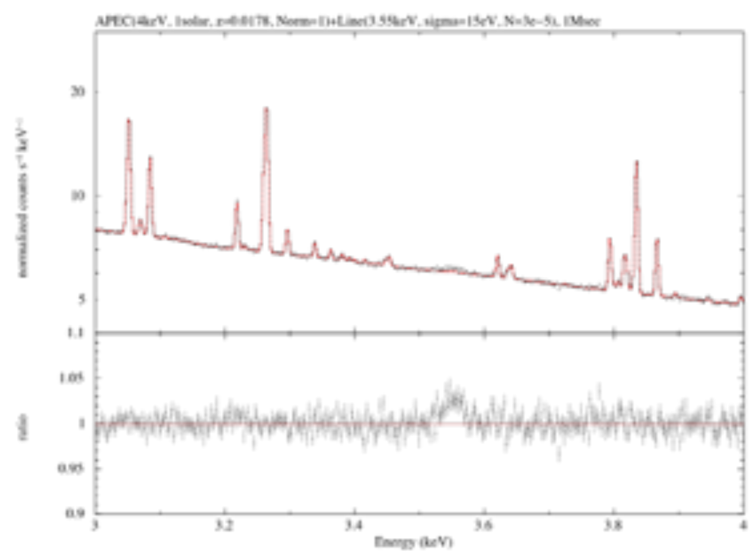

Introduction for X-ray search for dark matter

Feng 2010 ARAA, "Dark Matter Candidates from Particle Physics and Methods of Detection"

Table 1 Summary of dark matter particle candidates, their properties, and their potential methods of detection

	WIMPs	SuperWIMPs	Light $\tilde{G}$	Hidden DM	Sterile ν	Axions
Motivation	GHP	GHP	GHP/NPFP	GHP/NPFP	ν Mass	Strong CP
Naturally Correct Ω	Yes	Yes	No	Possible	No	No
Production Mechanism	Freeze Out	Decay	Thermal	Various	Various	Various
Mass Range	GeV-TeV	GeV-TeV	eV-keV	GeV–TeV	keV	μeV–meV
Temperature	Cold	Cold/Warm	Cold/Warm	Cold/Warm	Warm	Cold
Collisional				√		
Early Universe		√√		√		
Direct Detection	√√			√		√√
Indirect Detection	√√	√		√	√√	
Particle Colliders	√√	√√	√√	√		

The particle physics motivations are discussed in Section 2.2; GHP and NPFP are abbreviations for the gauge hierarchy problem and new physics flavor problem, respectively. In the last five rows, √√ denotes detection signals that are generic for this class of dark matter candidate and √ denotes signals that are possible, but not generic. "Early Universe" includes phenomena such as BBN (Big Bang nucleosynthesis) and the CMB (cosmic microwave background); "Direct Detection" implies signatures from dark matter scattering off normal matter in the laboratory; "Indirect Detection" implies signatures of late time dark matter annihilation or decay; and "Particle Colliders" implies signatures of dark matter or its progenitors produced at colliders, such as the Large Hadron Collider (LHC). See the text for details.

(1) Very low interaction → detectable exclusively from cosmic object.
(2) New particles discovered in the earth is the same dark matter in cosmic system ?

Provided by T. Tamura

THE ASTROPHYSICAL JOURNAL, 562:593–604, 2001 December 1

Provided by T. Tamura

DIRECT DETECTION OF WARM DARK MATTER IN THE X-RAY

KEVORK ABAZAJIAN,[1] GEORGE M. FULLER,[1] AND WALLACE H. TUCKER[1,2]

Received 2001 May 31; accepted 2001 July 31

ABSTRACT

We point out a serendipitous link between warm dark matter (WDM) models for structure formation on the one hand and the high-sensitivity energy range (1–10 keV) for X-ray photon detection on the *Chandra* and *XMM-Newton* observatories on the other. This fortuitous match may provide either a direct detection of the dark matter or the exclusion of many candidates. We estimate expected X-ray fluxes from field galaxies and clusters of galaxies if the dark matter halos of these objects are composed of WDM candidate particles with rest masses in the structure formation–preferred range ($\sim$1 to $\sim$20 keV) and with small radiative decay branches. Existing observations lead us to conclude that for singlet neutrinos (possessing a very small mixing with active neutrinos) to be a viable WDM candidate they must have rest masses $\lesssim$5 keV in the zero lepton number production mode. Future deeper observations may detect or exclude the entire parameter range for the zero lepton number case, perhaps restricting the viability of singlet neutrino WDM models to those where singlet production is driven by a significant lepton number. The Constellation X project has the capability to detect/exclude singlet neutrino WDM for lepton number values up to 10% of the photon number. We also consider diffuse X-ray background constraints on these scenarios. These same X-ray observations additionally may constrain parameters of active neutrino and gravitino WDM candidates.

Subject headings: dark matter — elementary particles — neutrinos — X-rays: diffuse background — X-rays: galaxies — X-rays: galaxies: clusters

Singlet or sterile neutrino

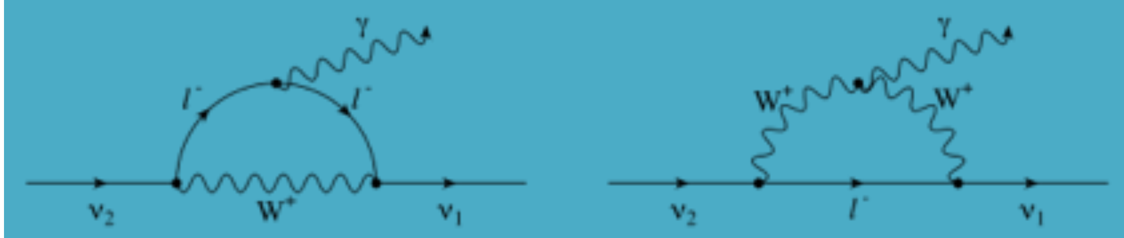

FIG. 2—Principal radiative decay modes for massive singlet neutrinos

Here θ is the vacuum mixing angle defined by an *effective* two-by-two unitary transformation between active ν_α species and a singlet species ν_s:

$$|\nu_\alpha\rangle = \cos\theta\,|\nu_1\rangle + \sin\theta\,|\nu_2\rangle\,,$$
$$|\nu_s\rangle = -\sin\theta\,|\nu_1\rangle + \cos\theta\,|\nu_2\rangle\,, \quad (6)$$

6.2 X-ray flux from Sterile Neutrinos (SN)

Provided by T. Tamura

Here we give some relations among dark matter parameters and observables given below and in § 5.1.

DM parameters		
DM mass within the fov	$M^{\rm fov}$	$M_\odot$
Luminosity and angular distance	$D_{\rm L}, D_{\rm A}$	pc
Surface mass density (column density)	$\Sigma_{\rm DM}$	$M_\odot$ pc^{-2}
$\nu_{\rm st}$ parameters		
decay rate	Γ	s^{-1}
Mixing angle	2θ	$\sin^2\theta = \frac{1}{4}\sin^2 2\theta$
SN mass	$m_{\rm SN}$	
Instruments/Observables		
X-ray flux from SN	$F_{\rm SN}$	photons cm^{-2} s^{-1}
X-ray flux from SN per solid angle	$f_{\rm SN}$	photons cm^{-2} s^{-1} str^{-1} (LU)

The followings are taken from [Abazajian et al.(2001)] (eq.1, eq.10).

$$L = \frac{E_\gamma}{m_{\rm SN}} M_{\rm DM}\Gamma, \quad (40)$$

$$= 4\pi D_L^2 F \quad (41)$$

$$\Gamma \simeq 6.8 \times 10^{-33} s^{-1} \left(\frac{\sin^2 2\theta}{10^{-10}}\right)\left(\frac{m_{\rm SN}}{1keV}\right)^5 \quad (42)$$

For the SN decay,

$$E_\gamma = m_{\rm SN}/2. \quad (43)$$

From [Loewenstein & Kusenko(2010)] (eq.2,3)

$$\Gamma \simeq 1.38 \times 10^{-32} s^{-1} \left(\frac{\sin^2 2\theta}{10^{-10}}\right)\left(\frac{m_{\rm SN}}{1keV}\right)^5 \quad (44)$$

Note that eq. 44 gives two times larger decay rate compared with eq. 42. [3]

$$F_{\rm SN} = 5.15 \times \sin^2\theta \times (\frac{m_{SN}}{\rm keV})^4 \times M_7^{\rm fov} d_{100}^{-2} \quad (45)$$

$$= 1.3 \times 10^{-9} \times \sin^2 2\theta \times \left(\frac{m_{SN}}{\rm keV}\right)^4 \times (M^{\rm fov}/M_\odot)(D_{\rm L}/Mpc)^{-2} {\rm photons cm^{-2} s^{-1}} \quad (46)$$

$$f_{\rm SN} = \frac{\Sigma_{\rm DM}\Gamma}{4\pi(1+z)^3 m_{\rm SN}} \quad (47)$$

Past observation targets

Table 2: Proposed and observed targets. R is integrated Radius. Papers: Aba2001; [Abazajian et al.(2001)], Boy2006a; [Boyarsky et al.(2006a)], Boy2008; [Boyarsky et al.(2008)], Boy2010a; [Boyarsky et al.(2010a)], Boy2010b; [Boyarsky et al.(2010b)], L10; [Loewenstein & Kusenko(2010)] L12; [Loewenstein & Kusenko(2012)], M10; [Mirabal(2010)].

paper	Target	D (Mpc)	R (pc)	Mass ($M_\odot$)	Σ ($M_\odot$ pc^{-2})	Ins.
Aba2001	Virgo	2.0e+01	5.6e+04	1.0e+13	1.0e+03	CXO
Aba2001	A85	2.3e+02	6.4e+05	3.5e+14	2.7e+02	CXO
Aba2001	Perseus	7.2e+01	2.0e+05	1.1e+14	8.4e+02	CXO
Aba2001	NGC 3198	1.8e+01	6.7e+04	4.3e+11	3.1e+01	Con-X
Aba2001	NGC 4123	2.2e+01	3.8e+04	7.0e+10	1.5e+01	Con-X
Boy2006a	CL/Coma (core)	98	–	–	—	XMM
Boy2006a	CL/Coma (outer)	98	–	–	—	XMM
Boy2006a	CL/Virgo (core)	20	–	–	—	XMM
Boy2006a	CL/Virgo (outer)	20	–	–	—	XMM
Boy2008	Cl/Bullet(Main)	1530	2.6e6	1.2e15	60	CXO
Boy2008	Cl/Bullet(Sub)	1530	2.8e5	5e13	210	CXO
Boy2008	dSph/Ursa Minor	0.066	270	3.3e7	150	
Boy2010a	M31/Core($r < 10'$)	0.78	2.5e3	(0.4-1.2)e10	200–600	XMM
Boy2010a	M31/Out($r \sim 40'$)	0.78	2e4	1.3e11	100	
Boy2010a	dSph/Fornax	0.138	560		55	
Boy2010a	dSph/Sculptor	0.079	100		150	
Boy2010b	MW/Center($\theta < 10$deg)	–	–	–	100–1000	Int/SPI
Boy2010b	MW/Core($\theta < 30$deg)	–	–	–	100–200	
Boy2010b	MW/Off($\theta > 90$deg)	–	–	–	50–80	
L09	dSph/Ursa Minor	0.069	400	(6^{+12}_{-3})e7	120	Suzaku
L10	Willman-I	0.038	55	2.6e6	210	CXO/AC
L12	ucd/Willman-I	0.038	100	4.2e6	135	CXO/AC
M10	ucd/Segue-1	0.023	67	6e5	43	Swift
Bul2014	Perseus	72	2.5e+5	1.49e14	76	EPIC
	Coma/Cen/Oph	~ 100	(2-4)e+5	(0.6-4.14)e14	60-80	EPIC
	'other CL'	z=0.1-0.4	-	-	-	EPIC
Boy2014	Perseus	72	2.5e+5	1.49e14	76	EPIC
	M31	0.78	-	-	-	EPIC

Provided by T. Tamura

Current limit on (Mass vs. mixing angle)

Tremaine-Gunn bound: DM dominated objects should not exceed the density of degenerate Fermi gas.

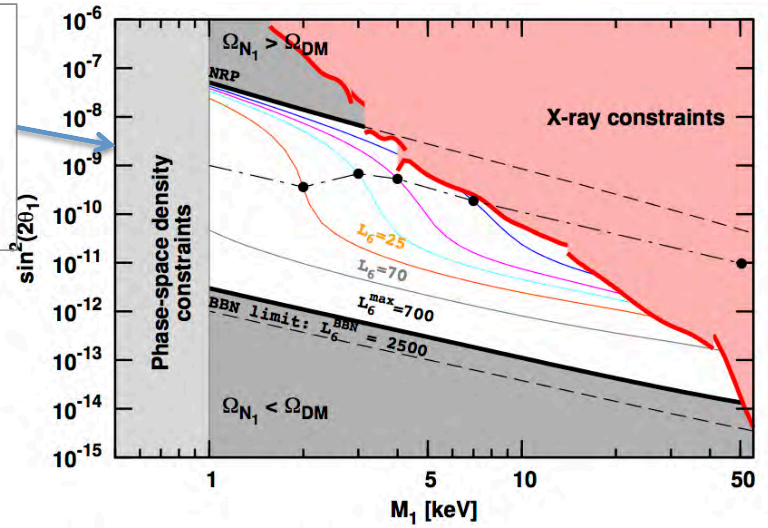

Figure 4: The allowed region of parameters for DM sterile neutrinos produced via mixing with the active neutrinos (*unshaded region*). The two thick black lines bounding this region represent production curves for nonresonant production (NRP) (*upper line*, $L_6 = 0$) and for resonant production (RP) (*lower line*, $L_6^{max} = 700$) with the maximal lepton asymmetry, attainable in the νMSM [53, 48]. The thin colored curves between these lines represent production curves for (*from top to bottom*) $L_6 = 8, 12, 16, 25$, and 70. The red shaded region in the upper right corner represents X-ray constraints [77, 78, 80, 88, 89] (rescaled by a factor of two to account for possible systematic uncertainties in the determination of DM content [86, 80]). The black dashed-dotted line approximately shows the RP models with minimal $\langle q \rangle$ for each mass, i.e., the family of models with the largest cold component. The black filled circles along this line are compatible with the Lyman-α bounds [90], and the points with $M_1 \leq 4$ keV are also compatible with X-ray bounds. The region below 1 keV is ruled out according to the phase-space density arguments [34]. Abbreviation: BBN, big bang nucleosynthesis.

Lines represent production curves for a various types of productions, $L_6=10^6$(Lepton number)/entropy. NRP: Nonresonance production, $L_6=0$)

Boyarsky+ 2009a

Bulbul et al. 2014 (B14)

Detection of unidentified line
in the Perseus cluster

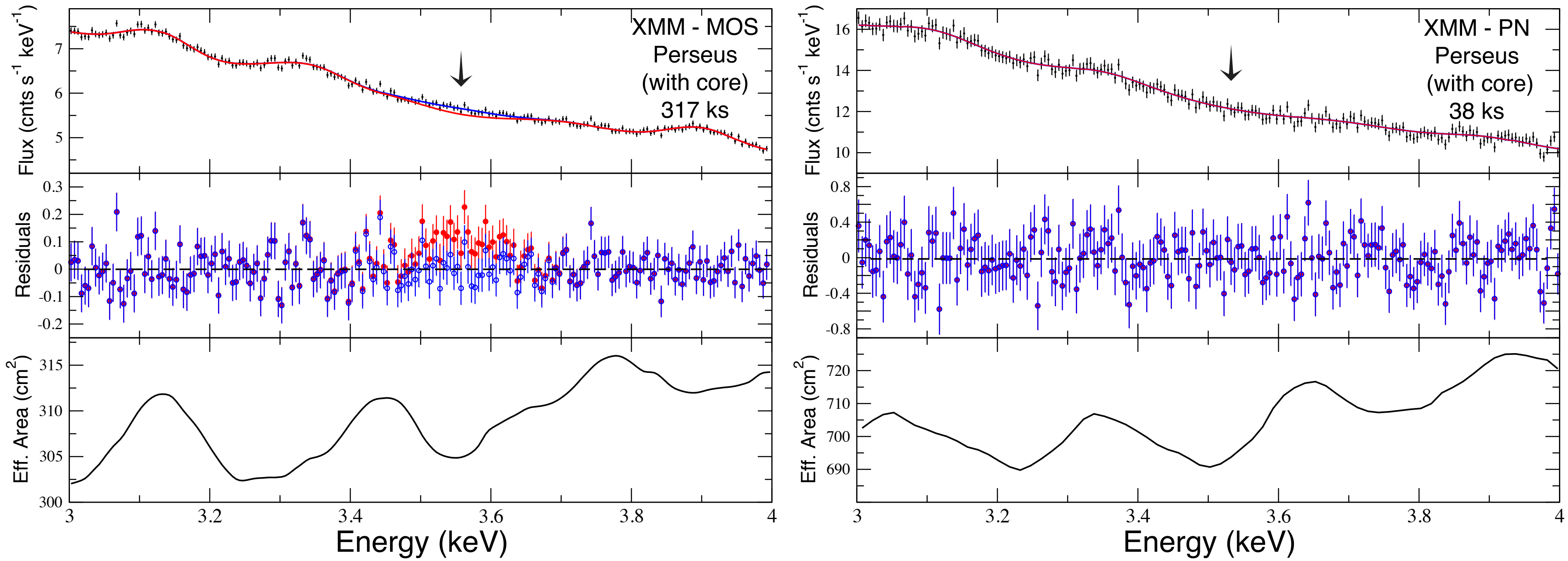

Figure 6. 3−4 keV band of the stacked MOS (left panel) and stacked PN (right panel) spectra of the Perseus cluster. The figures show the energy band, where a new spectral feature at 3.57 keV is detected. The Gaussian lines with peak values of the flux normalizations of K XVIII and Ar XVII estimated using AtomDB were included in the models. The red lines in the top panels show the model and the excess emission in both spectra. The blue lines show the total model after a Gaussian line is added, indicating that the unidentified spectral line can be modeled with a Gaussian.

Provided by T. Tamura

From Bulbul+2014

(6. Caveats) As intriguing as the dark-matter interpretation of our new line is, we should emphasize the significant systematic uncertainties affecting the line energy and flux in addition to the quoted statistical errors. The line is very weak, with an equivalent width in the full-sample spectra of only ~ 1 eV. Given the CCD energy resolution of ~ 100 eV, this means that our line is a ~ 1% bump above the continuum. This is why an accurate continuum model in the immediate vicinity of the line is extremely important; we could not leave even moderately significant residuals unmodeled. … Disentangling these possibilities is impossible at the present energy resolution and has to wait until the launch of *Astro-H*. The other systematic uncertainties mentioned above also have the low energy resolution as their root cause.

Provided by T. Tamura

Internal issues in Bulbul+ 2014

Provided by T. Tamura

Table 5
Properties of the Unidentified Emission Line

Sample		Inst. (1)	Energy (keV) (2)	Flux (10^{-6} photons cm^{-2} s^{-1}) (3)	χ^2 (dof) (4)	$\Delta\chi^2$ (Δ dof) (5)	M_{DM}^{proj}/D^2 (10^{10} $M_\odot$ Mpc^{-2}) (6)	$\sin^2(2\theta)$ (10^{-11}) (7)
Full sample	*XMM*	MOS	3.57 ± 0.02 (0.03)	$4.0^{+0.8}_{-0.8}$ $(^{+1.8}_{-1.2})$	564.8 (566)	22.8 (2)	1.82	$6.8^{+1.4}_{-1.4}$ $(^{+2.0}_{-3.0})$
		PN	3.51 ± 0.03 (0.05)	$3.9^{+0.6}_{-1.0}$ $(^{+1.0}_{-1.6})$	510.5 (564)	13.9 (2)	1.80	$6.7^{+1.7}_{-1.0}$ $(^{+2.7}_{-1.7})$
		PN	3.57*	$2.5^{+0.6}_{-0.7}$ $(^{+1.0}_{-1.1})$	510.5 (564)	11.2 (1)	1.80	$4.3^{+1.2}_{-1.0}$ $(^{+1.8}_{-1.7})$
Coma + Centaurus + Ophiuchus	*XMM*	MOS	3.57*	$15.9^{+3.4}_{-3.8}$ $(^{+6.7}_{-5.5})$	562.3 (569)	17.1 (1)	2.68	$18.2^{+4.4}_{-3.9}$ $(^{+12.6}_{-11.5})$
		PN	3.57*	<9.5	377.8 (387)	…	…	<10.9
Perseus (without the core)	*XMM*	MOS	3.57*	$21.4^{+7.0}_{-6.3}$ $(^{+11.2}_{-10.5})$	596.1 (574)	12.8 (1)	2.82	$23.3^{+7.6}_{-6.9}$ $(^{+12.2}_{-11.5})$
		PN	3.57*	<16.1	539.1 (553)	…	…	<17.6
Perseus (with the core)	*XMM*	MOS	3.57*	$52.0^{+24.1}_{-15.2}$ $(^{+37.0}_{-21.3})$	613.8 (574)	15.7 (1)	2.89	$55.3^{+25.5}_{-15.9}$ $(^{+39.3}_{-22.6})$
		PN	3.57*	<17.7	539.4 (554)	…	…	<18.8
All other clusters	*XMM*	MOS	3.57*	$2.1^{+0.4}_{-0.5}$ $(^{+0.8}_{-0.8})$	547.2 (573)	16.5 (1)	1.08	$6.0^{+1.1}_{-1.4}$ $(^{+2.3}_{-2.3})$
		PN	3.57*	$2.0^{+0.3}_{-0.5}$ $(^{+0.3}_{-0.8})$	741.9 (751)	15.8 (1)	1.15	$5.4^{+0.8}_{-1.3}$ $(^{+1.3}_{-2.1})$
Perseus	*Chandra*	ACIS-S	3.56 ± 0.02 (0.03)	$10.2^{+3.7}_{-3.5}$ $(^{+4.8}_{-4.7})$	201 (197)	11.8 (2)	0.72	$40.1^{+14.5}_{-13.7}$ $(^{+18.9}_{-18.2})$
		ACIS-I	3.56*	$18.6^{+7.8}_{-8.0}$ $(^{+12.0}_{-16.0})$	152.6 (151)	6.2 (1)	1.86	$28.3^{+11.8}_{-12.1}$ $(^{+18.2}_{-24.3})$
Virgo	*Chandra*	ACIS-I	3.56*	<9.1	189.1 (155)	…	2.41	<10.5

Notes. Columns 2 and 3 are the measured rest energy and flux of the unidentified line in the units of photons cm^{-2} s^{-1} at the 68% (90%) confidence level. The energies with asterisks are frozen to the indicated values; Columns 4 and 5 show the χ^2 before the line is added to the total model and change in the χ^2 when an additional Gaussian component is added to the fit; Column 6 is the weighted ratio of mass to distance squared of the samples; and Column 7 shows the mixing angle limits measured in each sample. Reported constraining limits are 90% confidence upper limits. Energies marked with star symbols were held fixed during the model fitting.

1. MOS/PN fluxes are inconsistent except for 'All other'.
2. Perseus center flux is ~10 times larger than others in terms of DM decay-rate.
3. Detected line are very weak. Fluxes are always < 3 eV in EW or a few % in excess of the continuum.
4. Line centers are not formally consistent among 3 data sets.

Provided by T. Tamura

2014 Detections (Bulbul+; Boyarsky+)

Sample	Instrument	Energy	Flux *f	Δχ2 (Δdof)	Comments
Coma+Cen +Oph	*XMM/MOS*	*3.57 fix*	*15.9+3.4-3.8*	*17.1 (1)*	**1*
Perseus (r>1')	*MOS*	*3.57 fix*	*21.4*	*12.8*	**1*
Perseus (full)	*MOS*	*3.57 fix*	*52.0 +24.1-15.2*	*15.7*	**1*
69 clusters	*MOS*	*3.57 fix*	*2.1 +0.4,-0.5*	*16.5*	*< 1/10 of the*
Perseus	*CXO/ACIS-S*	*3.56+- 0.02*	*10.2+3.7-4.7*	*11.8*	*Suggested also in ACIS-I*
Virgo	*ACIS-I*	*3.56 fix*	*< 9.1*	*…*	*No detection*
Perseus (off-	*MOS*	*3.50+0.044-0.*	*7.0+2.6-2.3*	*9.1*	*R>20'*
M31 center	*MOS*	*3.53+- 0.025*	*4.9 +1.6-1.3*	*13*	
MW center	*MOS*	*3.54 +- 0.01*	*29+-5*	*(~ 6σ)*	*No detection*

*f 1e-6 cts/cm2/s, *1 No detection in PN

T. Tamura et al. 2015

Suzaku search for unidentified lines

Independent check of 3.5 keV line from the Perseus Cluster

by Tamura et al. 2015 PASJ

Publ. Astron. Soc. Japan (2015) 00 (0), 1–16
doi: 10.1093/pasj/psu156
Advance Access Publication Date: 2015 0

An X-ray spectroscopic search for dark matter in the Perseus cluster with Suzaku

Takayuki TAMURA,* Ryo IIZUKA, Yoshitomo MAEDA, Kazuhisa MITSUDA, and Noriko Y. YAMASAKI

Institute of Space and Astronautical Science, Japan Aerospace Exploration Agency, 3-1-1 Yoshinodai, Chuo-ku, Sagamihara, Kanagawa 229-8510, Japan

*E-mail: tamura.takayuki@jaxa.jp

Received 2014 November 10; Accepted 2014 December 13

Provided by T. Tamura

Suzaku (Japan-US X-ray mission)

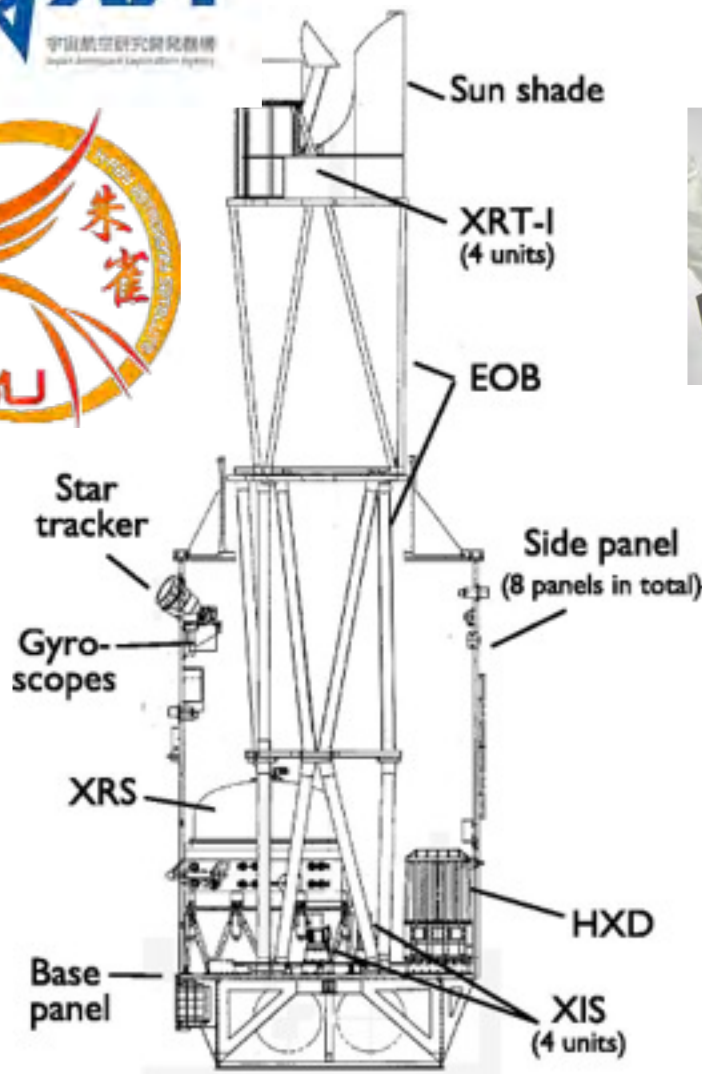

Mitsuda et al. 2007


XRT

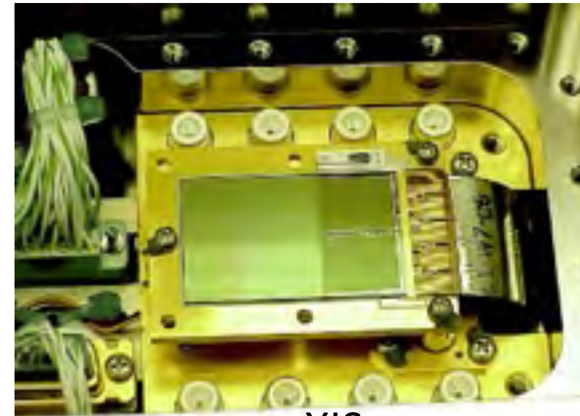
XIS

XIS (X-ray Imaging Spectrometer)

- **High sensitivity, 17’x 17’(0.5-12keV)**
- Spatial resolution is ~ 1.5 arcmin.
- **Good energy response and calibration.**

HXD (Hard X-ray Detector)

- Broad band in 15 - 600 keV

T. Tamura et al. 2015

Suzaku obs. of the Perseus cluster

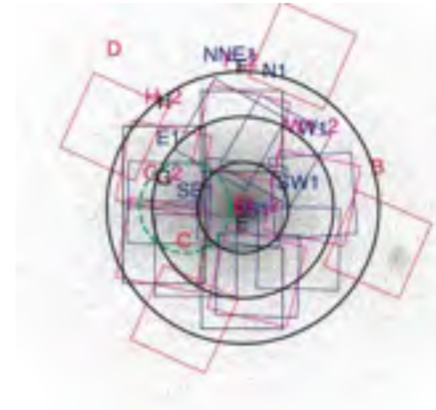

(1) Calibration (center) and Key project (large region) target

—> **500 ksec** in total

(2) 1st detection of X-rays from rare-metals (Mn & Cr), (Tamura+ 2009)

—> Good weak line sensitivity

(3) Gas Bulk Motion Measured (Tamura + 2014)

—> Good understanding of response

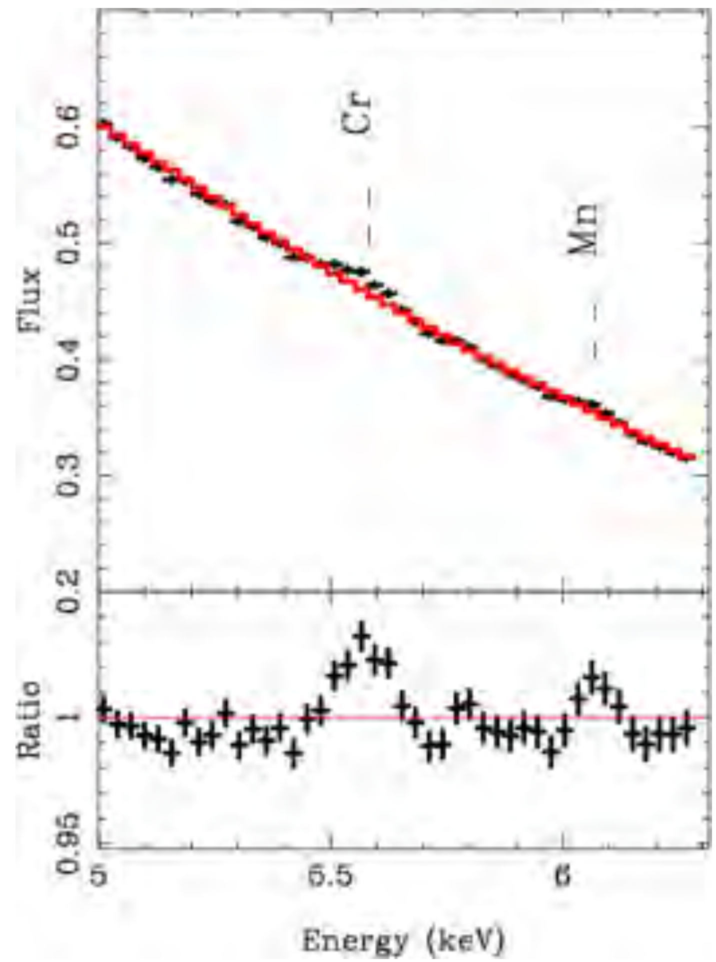

- Ozawa+ 2009, Uchiyama+2009, Nishino+2010, Simionescu+ 2011,2012, Matsushita+2013, Werner+ 2014, etc.,

T. Tamura et al. 2015

XMM vs. Suzaku in expected photon counts

Table 6: *Suzaku* XIS and *XMM-Newton* EPIC observations. Areas are for the enrgy of 3.5 keV. EPIC exposures are those of Bulbul et al. (2014). The MOS and FI exposures are sums of CCD.

Detector	Area (cm^2)	FOV ($arcmin^2$)	exp (ks)	Area× exp ()	Area× exp × FOV ()	
MOS	300	710	317	95.1K	67.5M	XMM-Newton
PN	700	710	38	26.6K	18.9M	
XIS/FI	260	320	1040	270K	86.5M	Suzaku
XIS/BI	260	320	530	138K	44.1M	
total	-	-	-	408K	131M	

In terms of exposure x area (photon counts), the Suzaku obs. is 4 times larger than XMM/Bulbul+2014.

Suzaku XIS Au M-edges structures

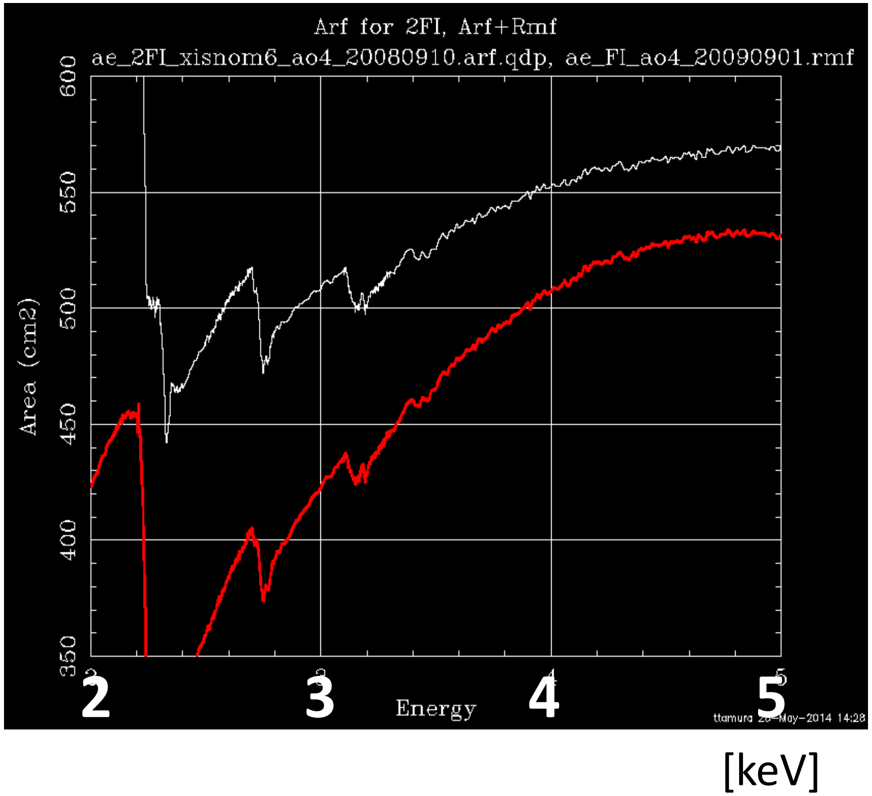

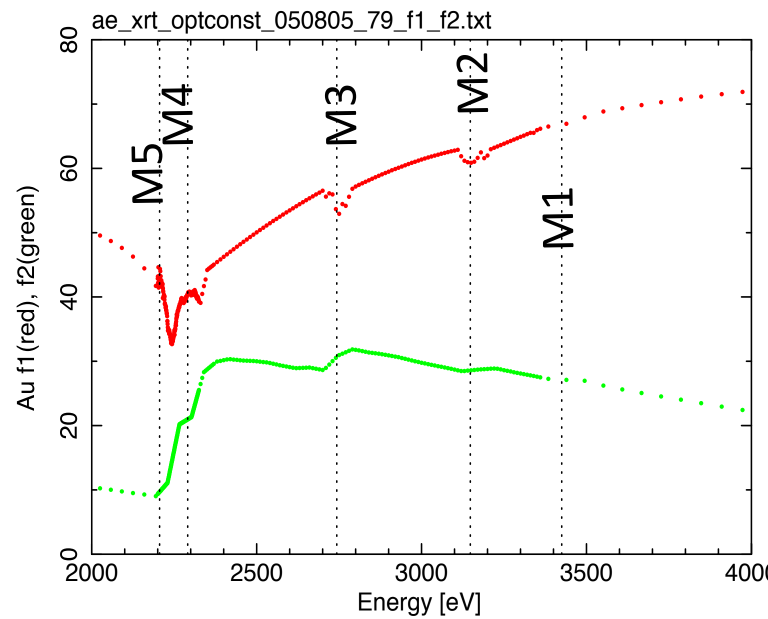

Effective areas of Telescope+CCD and Telescope used in the response.

Measurements of Au reflection parameters (f1,f2). These data are used to make Suzaku responses (Iizuka+, priv. comm.). Note that E>3.4keV energy steps becomes coarse.

Provided by T. Tamura

Ground calibration for the optical constant on mirror reflector

Tamura K.++ 2006

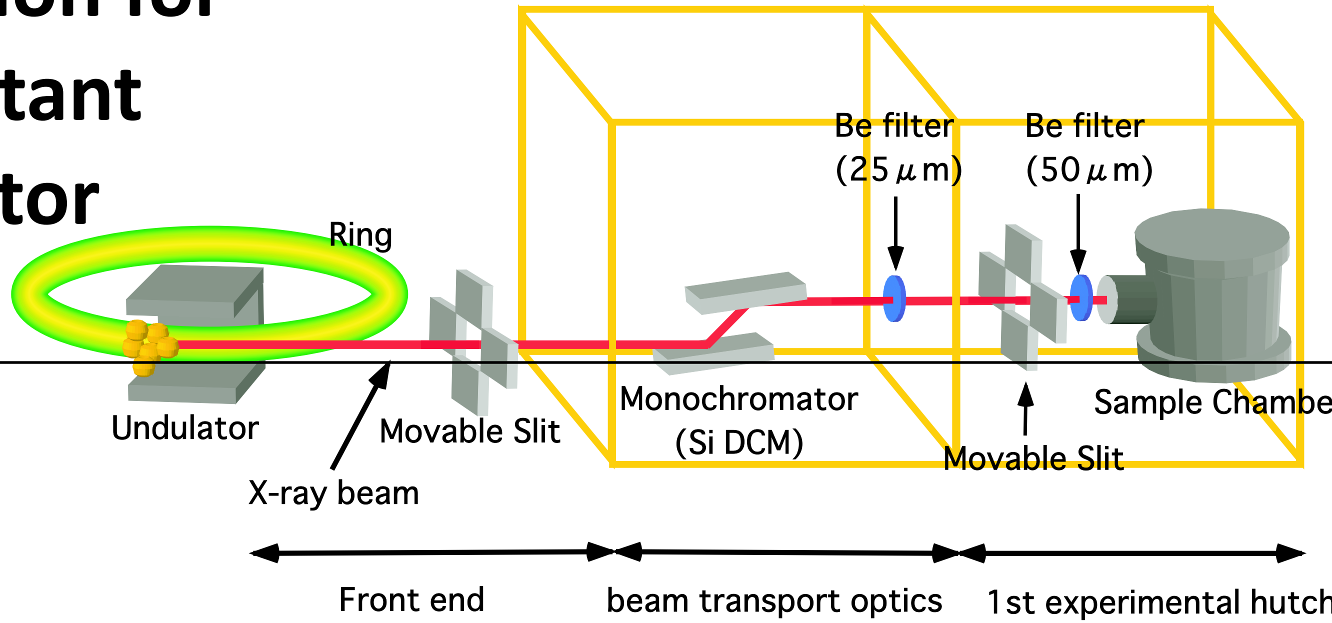

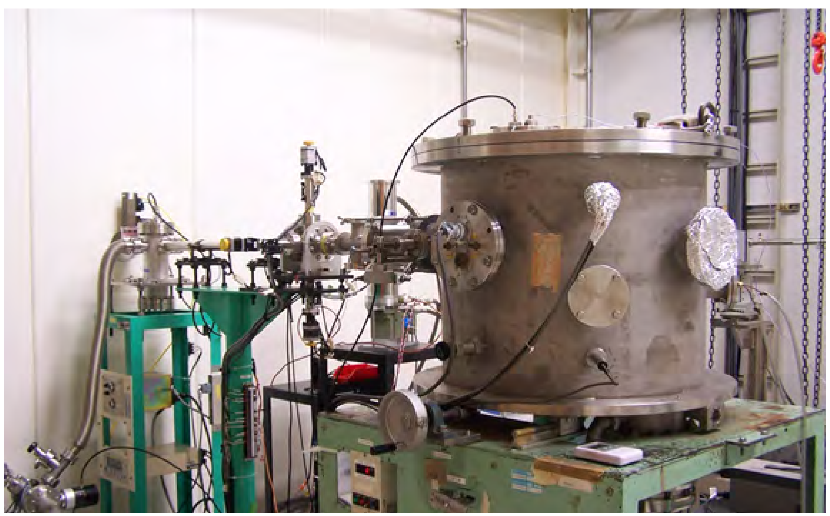

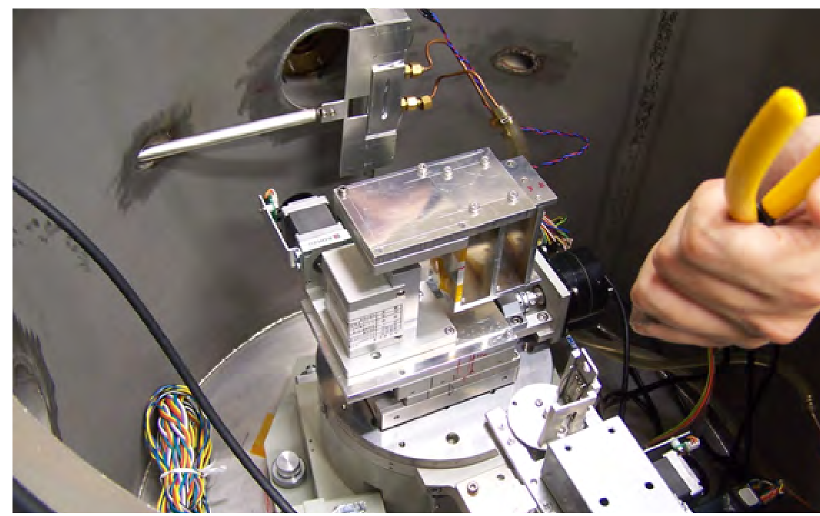

one witness sample —> 175 foil pairs

Provided by T. Tamura

Modeling of the response feature with the Crab

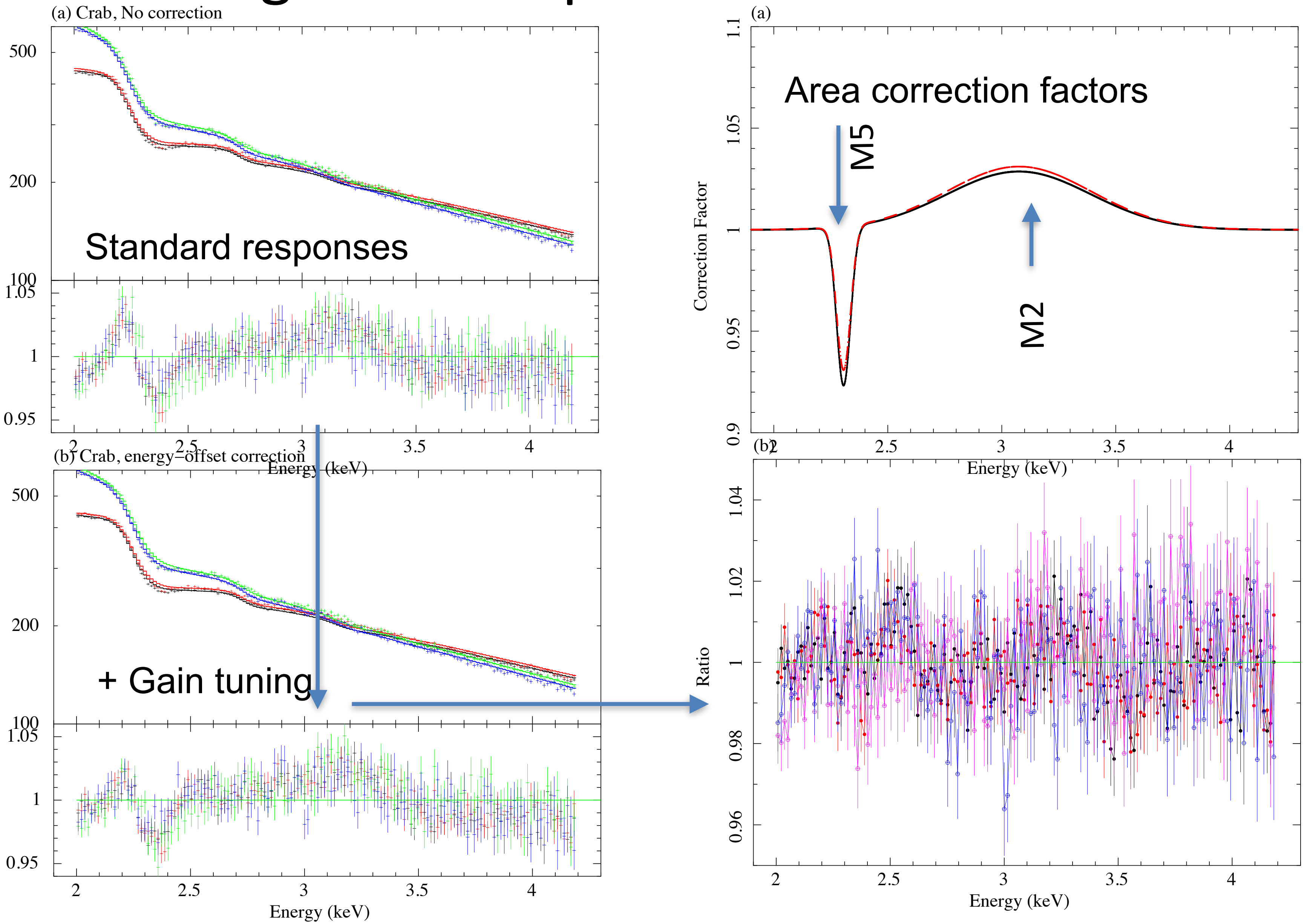

T. Tamura et al. 2015

T. Tamura et al. 2015

Systematic error on line equivalent width

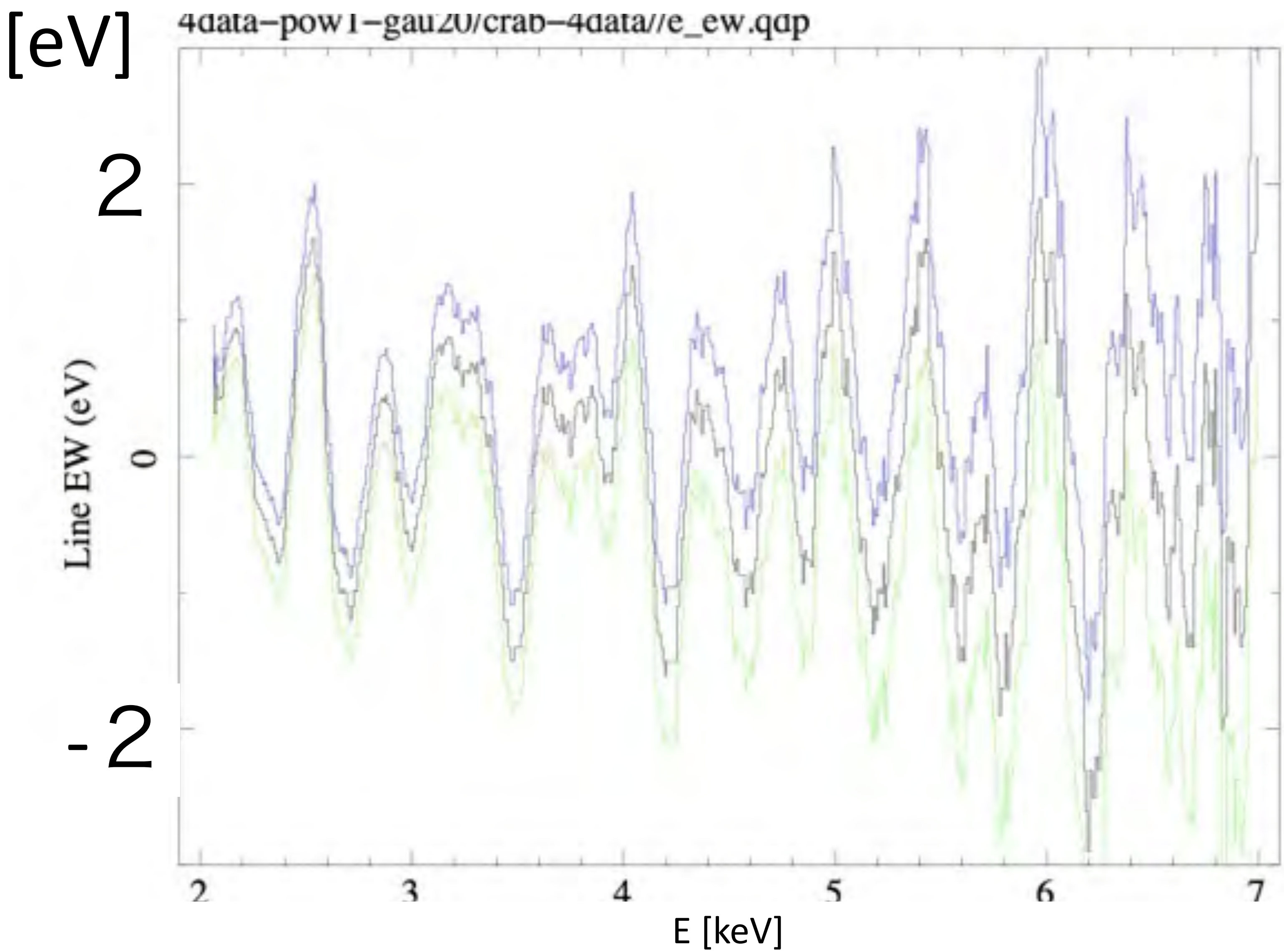

The Perseus *Suzaku* spectra

T. Tamura et al. 2015

R<2’

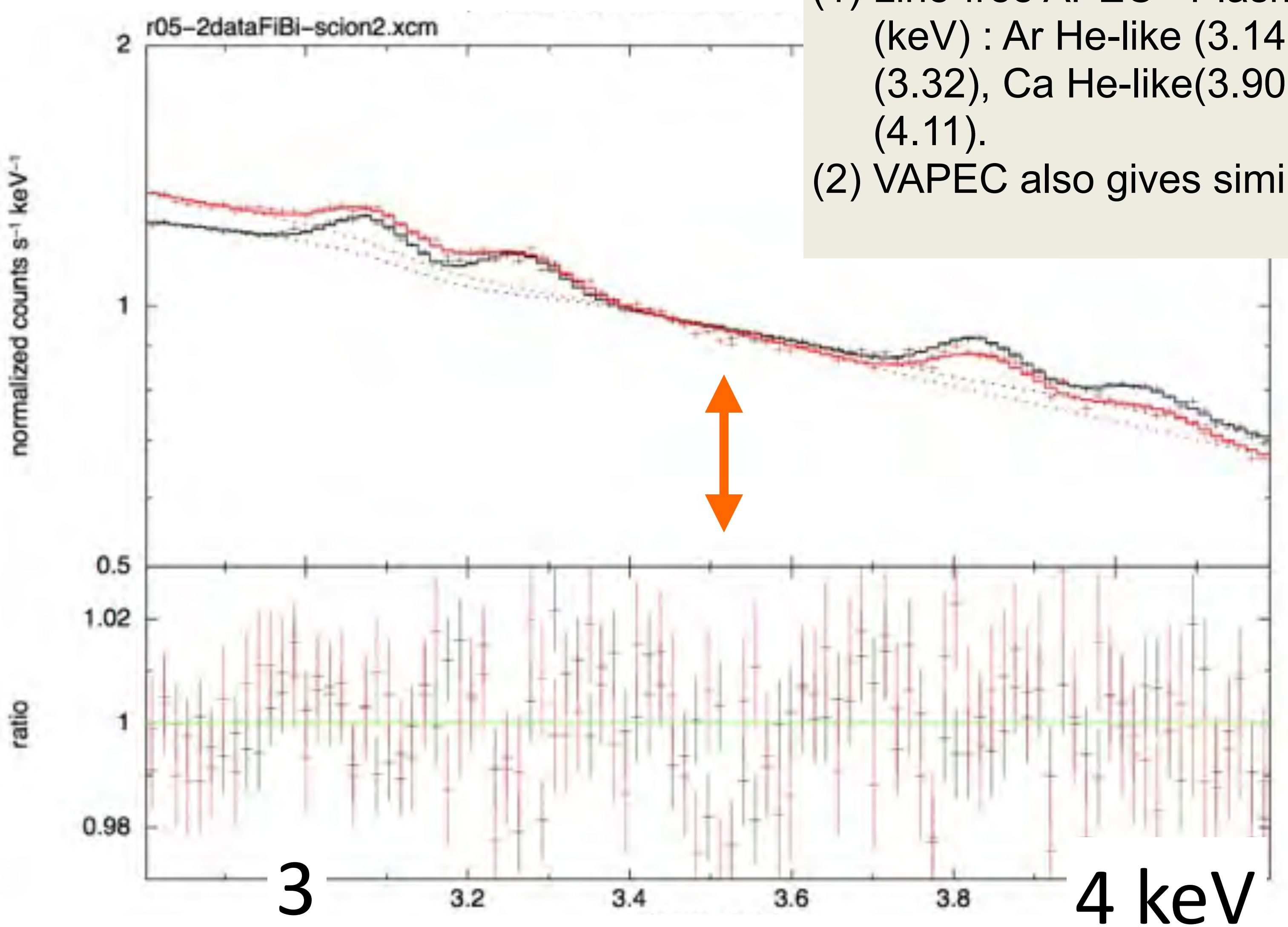

(1) Line-free APEC+ Plasma lines (keV) : Ar He-like (3.14), Ar H-like (3.32), Ca He-like(3.90), Ca H-like (4.11).
(2) VAPEC also gives similar fit result.

Possible Dark matter line at 3.57± 0.02 keV (rest-frame; Bulbul+, MOS) → 3.51 (observed) keV

2’<R<4’

T. Tamura et al. 2015

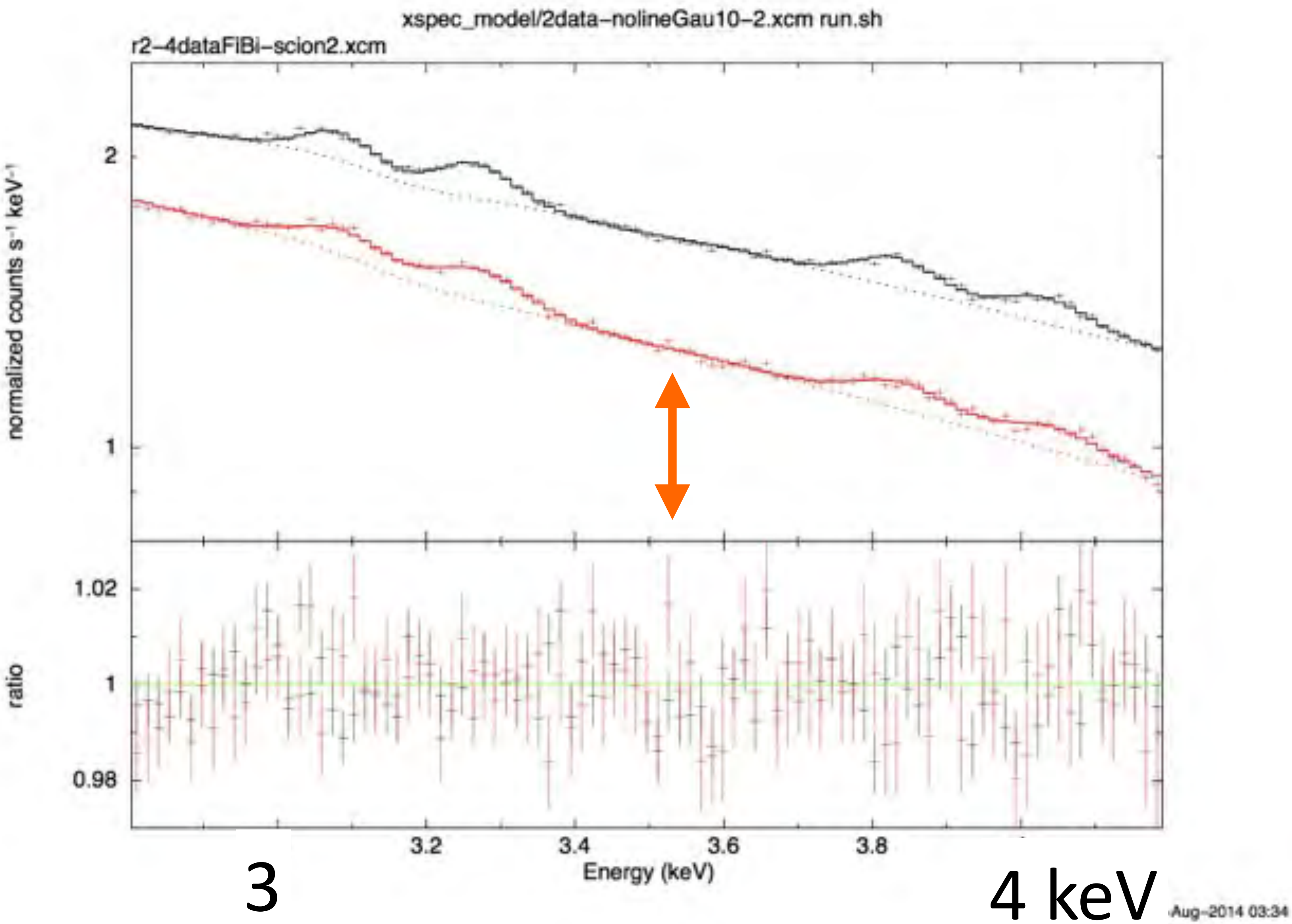

3

4 keV

R<10' spectra with the 3.5keV Line (B14 flux)

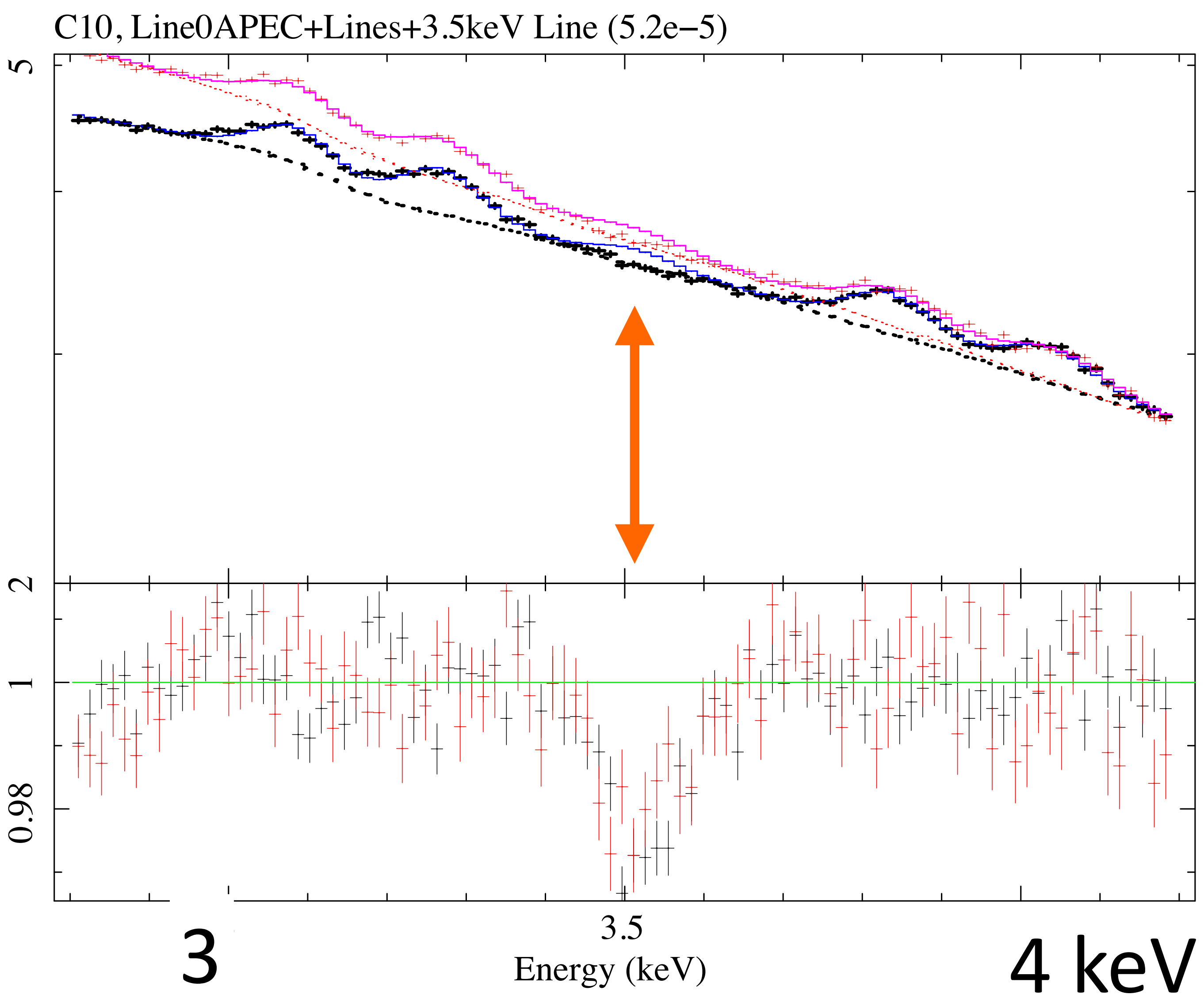

T. Tamura et al. 2015

The best ICM spectra

T. Tamura et al. 2015

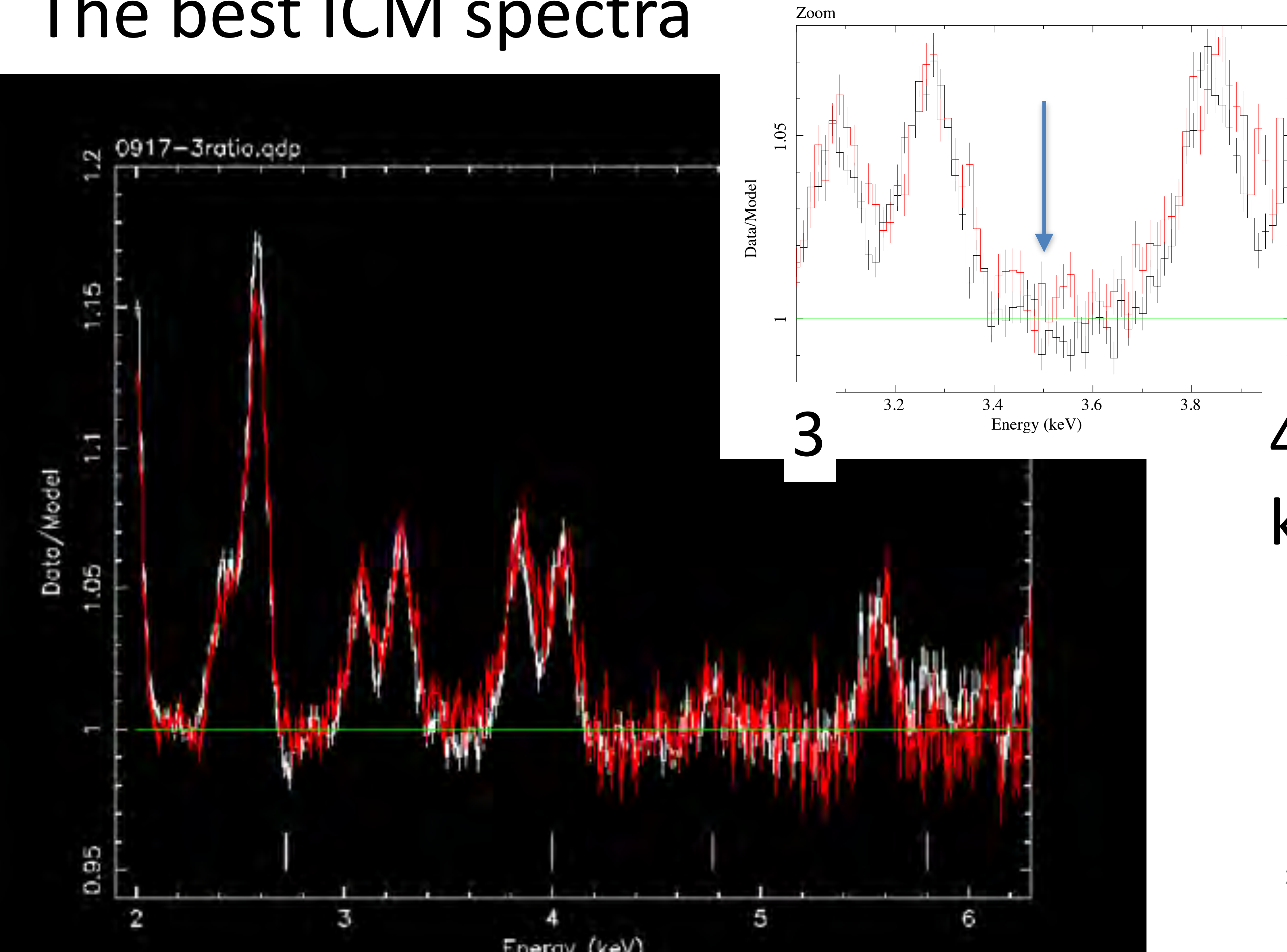

3

4 keV

Suzaku Limits on Line fluxes

Line search from the Perseus spectra.
Black line: possible line flux in the Perseus.
Red line: systematic uncertainties on the line flux from the Crab fitting.
At the DM line position (3.5 keV), statistical limit < 1/5 XMM detection, systematic limit ~ 2eV ~2/3 of the XMM detection.

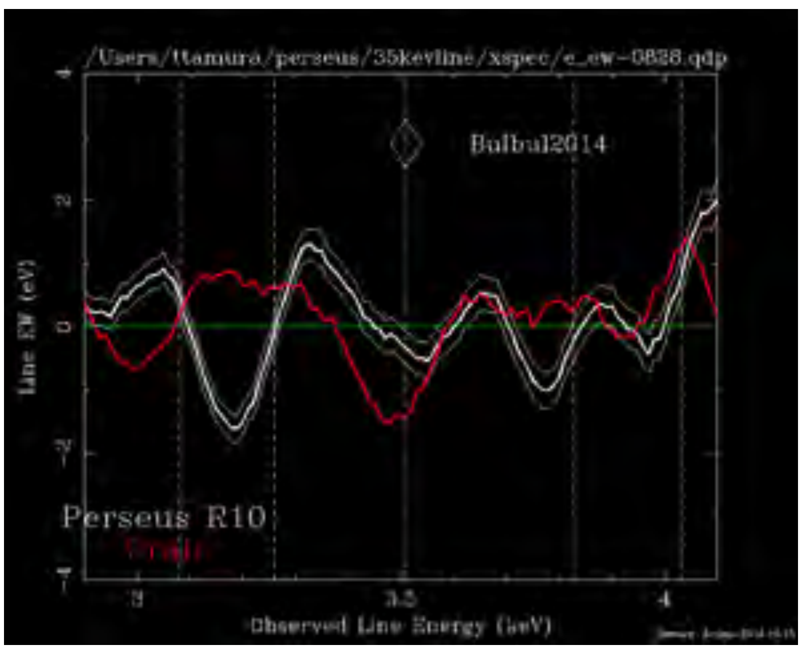

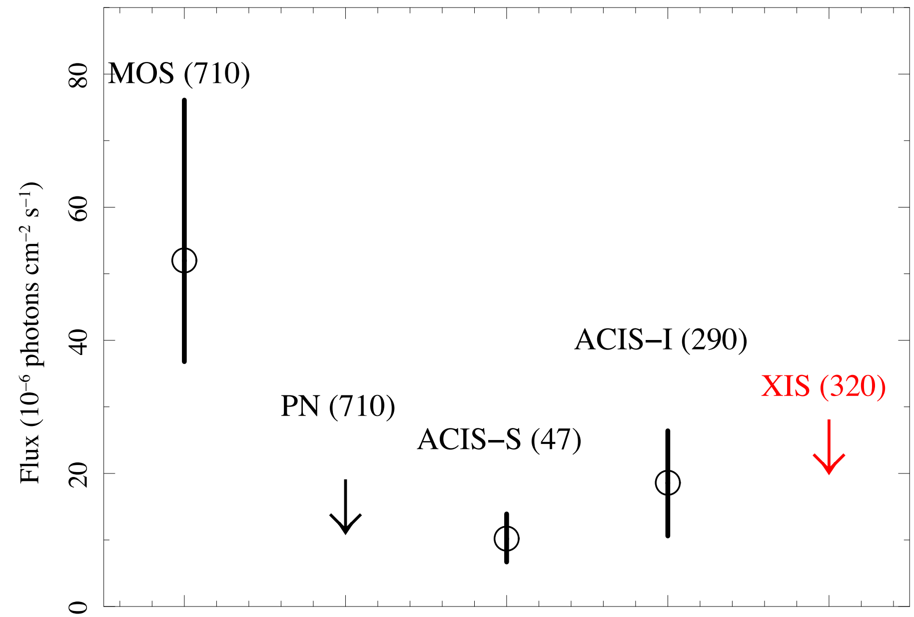

Line fluxes in the Perseus center at 3.51~keV. The XMM and Chandra values are taken from Bulbul+ (2014) The detector name (sizes of spectral extraction in arcmin^2) are shown.

T. Tamura et al. 2015

Suzaku deep search for unidentified lines Using the Milky Way by Sekiya et al. 2015

A Search for a keV Signature of Radiatively Decaying Dark Matter with Suzaku XIS Observations of the X-ray Diffuse Background

Norio SEKIYA, Noriko Y. YAMASAKI, and Kazuhisa MITSUDA

Institute of Space and Astronautical Science, Japan Aerospace Exploration Agency, 3-1-1 Yoshinodai, Sagamihara, Chuo-ku, Kanagawa 252-5210, Japan

*E-mail: yamasaki@astro.isas.jaxa.jp

Received ; Accepted

Abstract

We performed the deepest search for an X-ray emission line between 0.5 and 7 keV from non-baryonic dark matter with the Suzaku XIS. Dark matter associated with the Milky Way galaxy was selected as the target to obtain the best signal-to-noise ratio. From the Suzaku archive, we selected 187 data sets of blank sky regions which were dominated by the X-ray diffuse background. The data sets were from 2005 to 2013. Instrumental responses were adjusted by multiple calibration data sets of the Crab Nebula. We also improved the technique of subtracting lines of instrumental origin. These energy spectra were well described by X-ray emission due to charge exchange around the Solar System, hot plasma in and around the Milky Way and superposition of extra-galactic point sources. A signal of a narrow emission line was searched for, and the significance of detection was evaluated in consideration of the blind

Provided by T. Tamura

Dark matter column density

Table 10: Mass distritbuion parameters. Cluster NFW parameters are taken from kT-M relation in Vikhlinin 2009. $r_s/R_{500} = 3$ is assumed for clusters. NFW parameters (r_s, ρ_s) for dwarf galaxies are taken from [Strigari et al.(2008b)] (Fig.1) and Strigari et al. 2007. Those of MW are from [Boyarsky et al.(2008)] and [Klypin et al.(2002)].

name	D_A (pc)	r_s (pc)	ρ_s ($M_\odot$ pc^{-3})	$r_s\rho_s$ ($M_\odot$ pc^{-2})	1′ (pc)
Perseus	7.50e+07	4.27e+05	1.00e-03	4.27e+02	2.18e+04
Coma	9.62e+07	4.90e+05	1.01e-03	4.95e+02	2.80e+04
Virgo	1.63e+07	2.53e+05	1.00e-03	2.53e+02	4.74e+03
Ursa-majorII	3.2e+04	6.0e+02	1.5e-01	9.0e+01	9.3e+00
Coma-Berenices	4.4e+04	3.0e+02	2.5e-01	7.5e+01	1.3e+01
Will-I	3.8e+04	2.0e+02	3.0e-01	6.0e+01	1.1e+01
Ursa-Minor	6.6e+04	1.5e+02	6.0e-01	9.0e+01	1.9e+01
Draco	8.0e+04	8.0e+02	6.0e-02	4.8e+01	2.3e+01
MW/Favoured	8.0e+03	2.2e+04	4.9e-03	1.1e+02	2.3e+00
MW/maximum-disk-A	8.0e+03	4.6e+04	6.0e-04	2.8e+01	2.3e+00
MW/maximum-disk-B	8.0e+03	2.3e+04	3.1e-03	7.1e+01	2.3e+00

Dark matter concentration (galaxy and cluster center) → Gas and stars concentrate → X-ray emission, absorption
Galaxy center → Dark matter has cusp or core ?

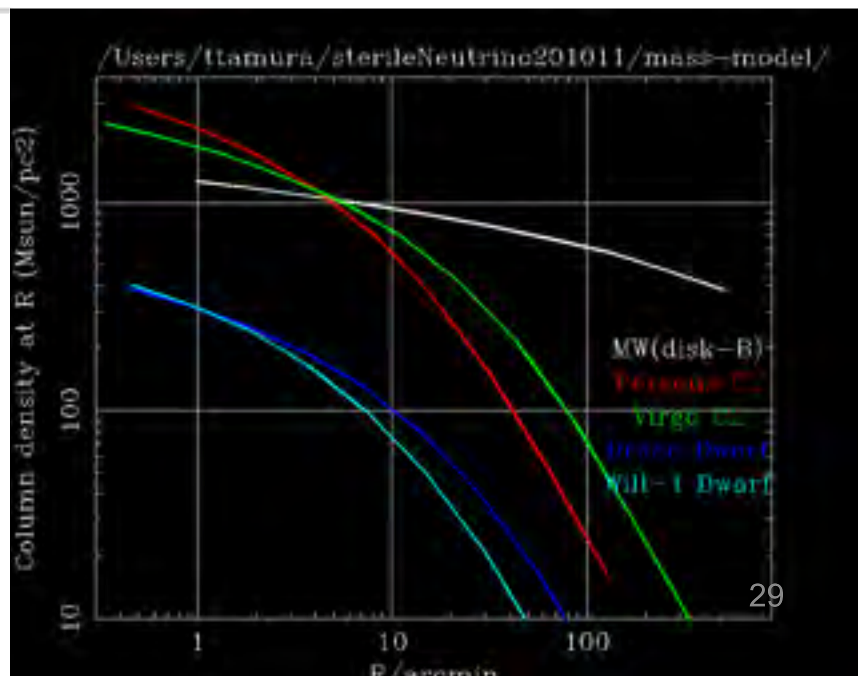

Direction for DM line search

Sekiya et al. 2015

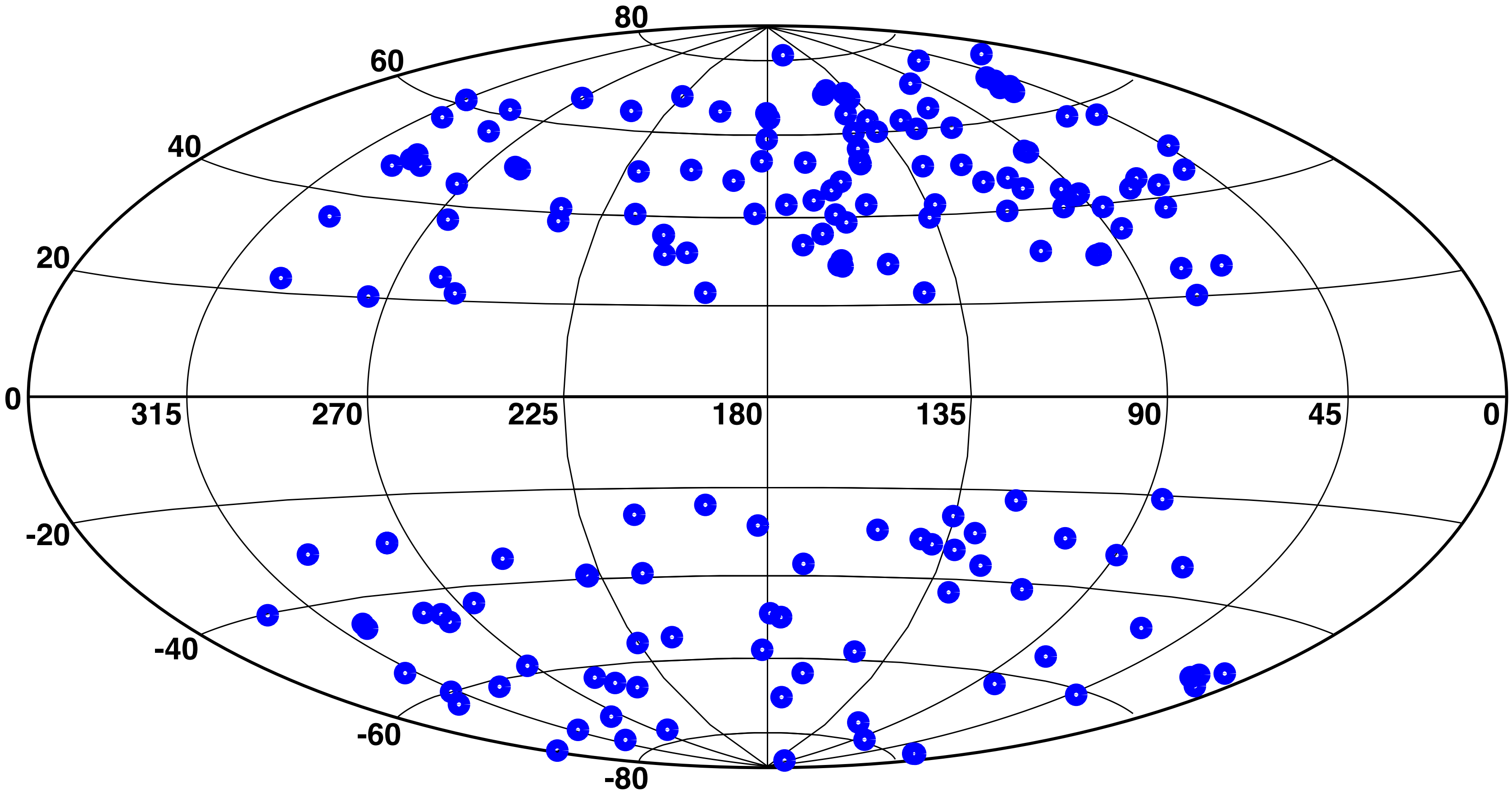

Fig. 1. 187 regions used to search for a keV signature of DM from Suzaku archival data. These are plotted on the all sky map with the Galactic coordinate system centered at the Galactic anti-center.

Sekiya et al. 2015

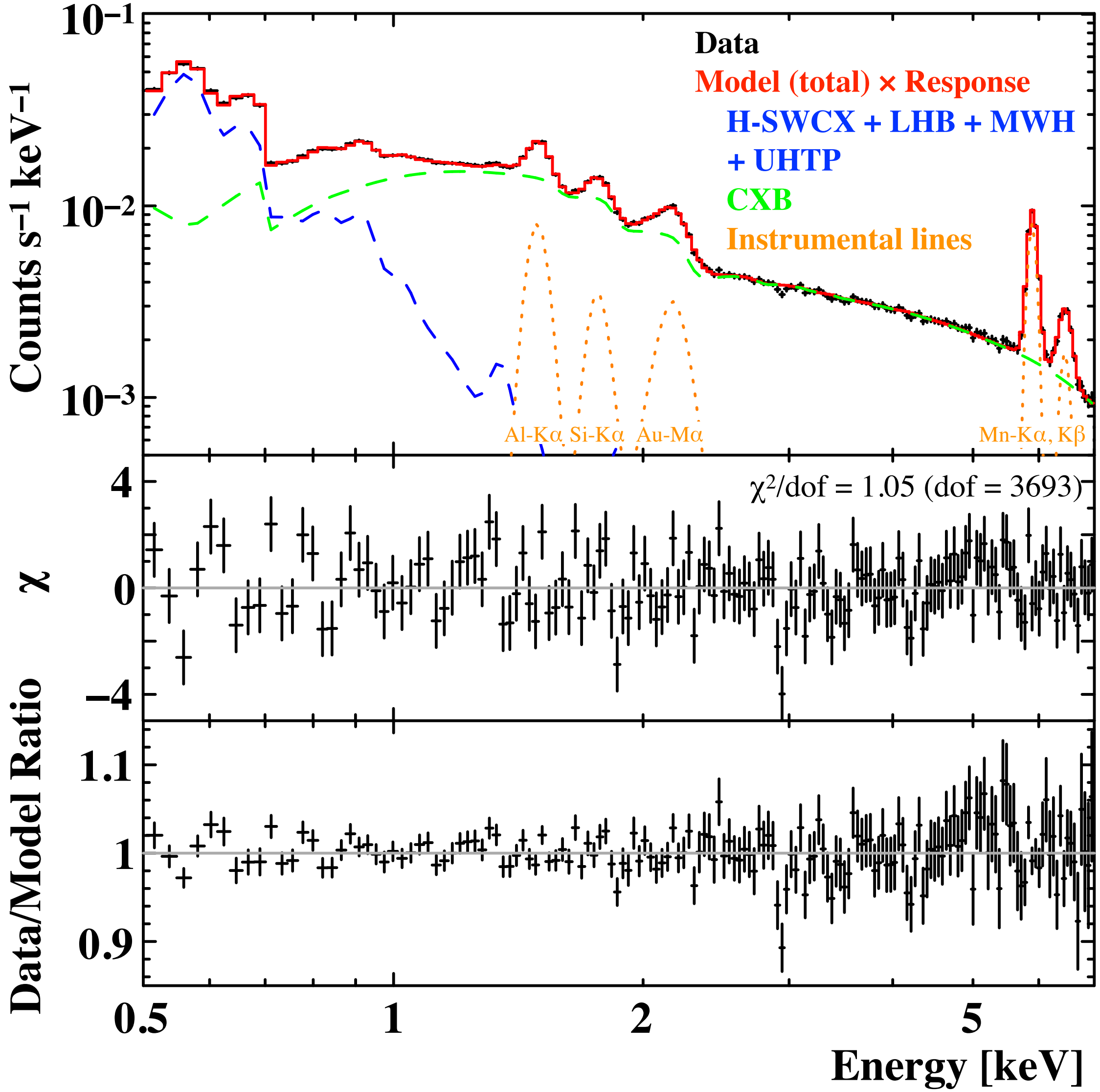

Fig. 2. Exposure-time-weighted average of the 25 stacked XDB energy spectra from 2005 to 2013 and its best-fit model convolved with the corrected response. Sub-components of the model are represented by blue dashed (XDB in the Milky Way (1)+(2)+(4)), green dashed (CXB (3)) and orange dotted (instrumental origin) lines.

Stacked spectra

No significant residuals

Sekiya et al. 2015

Upper limit for DM line

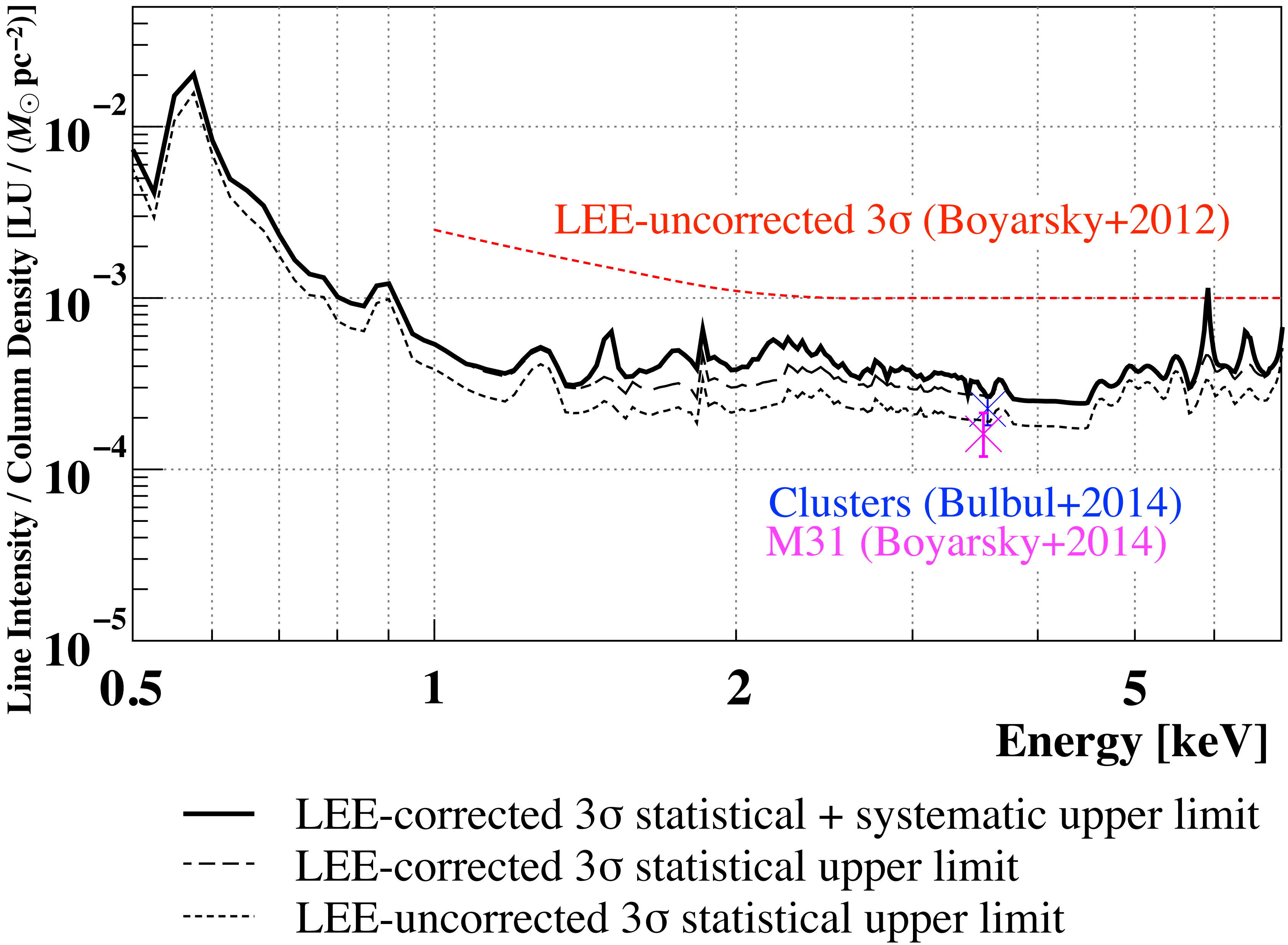

Sekiya et al. 2015

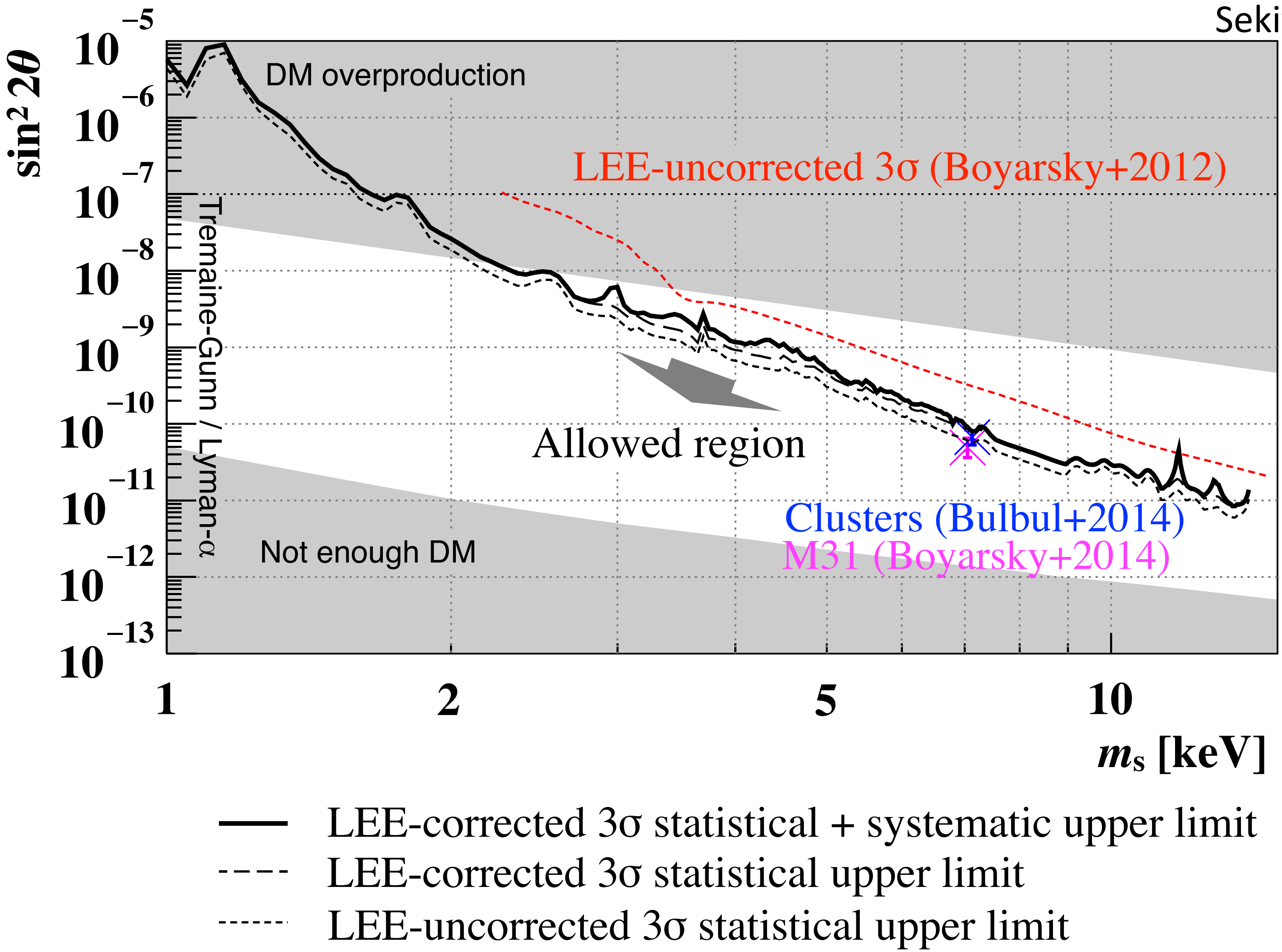

Fig. 6. Constraints on the sterile neutrino mass $m_{\rm s}$ and mixing angle $\sin^2 2\theta$ by this and previous works. The definition of lines and marks are the same as in Fig. 5. The grey shaded regions are excluded by the production theories of sterile neutrinos in the νMSM.

Summary of Suzaku Results

- Loewenstein, M., Kusenko, A., & Biermann, P. L. (2009) ApJ
"New Limits on Sterile Neutrinos from Suzaku Observations of the Ursa Minor Dwarf Spheroidal Galaxy"

- Kusenko, A., Loewenstein, M., & Yanagida, T. (2013) Physical Review D
"Moduli dark matter and the search for its decay line using Suzaku X-ray telescope"

- Tamura, T., Iizuka, R., Maeda, Y., Mitsuda, K. & Yamasaki, Y. N. (2015) PASJ
"An X-ray spectroscopic search for dark matter in the Perseus cluster with Suzaku"

- Sekiya, N., Yamasaki, Y. N. & Mitsuda, K. (2015) arXiv:1504.02826
"A Search for a keV Signature of Radiatively Decaying Dark Matter with Suzaku XIS Observations of the X-ray Diffuse Background"

No significant detection of Sterile neutrino signal

Future with ASTRO-H

Provided by T. Tamura

- High Resolution Spectroscopy with a large effective area

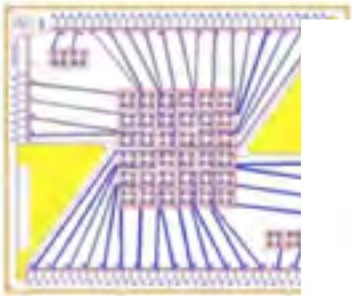

814 μm
6x6 array
34 pixel readout
50 mK

Takahashi, T> & AH collaborations

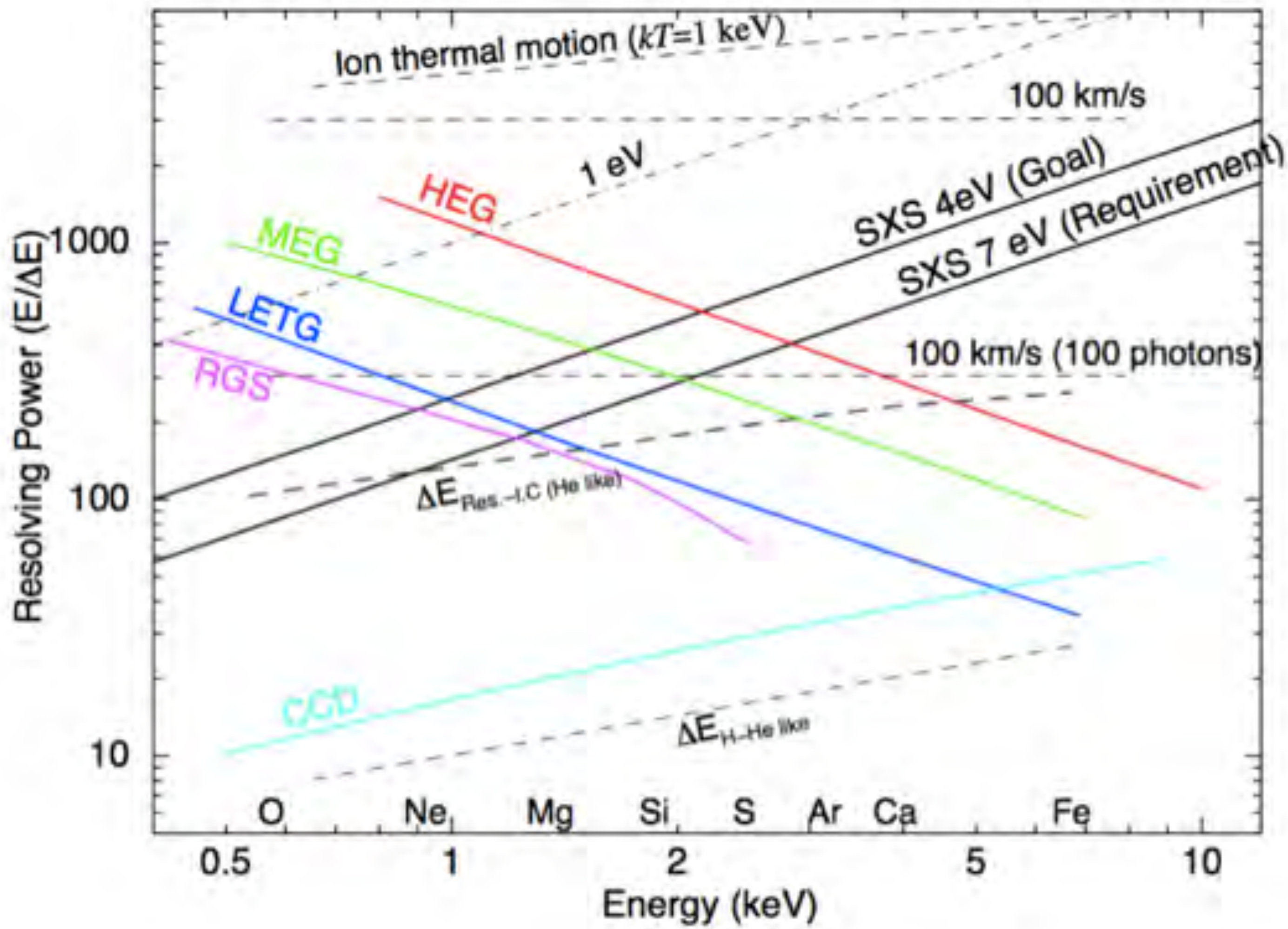

R. Petre

Astro-H SXS

- High Resolution Spectroscopy with a large effective area

210cm^2@6keV

Takahashi, T> & AH collaborations

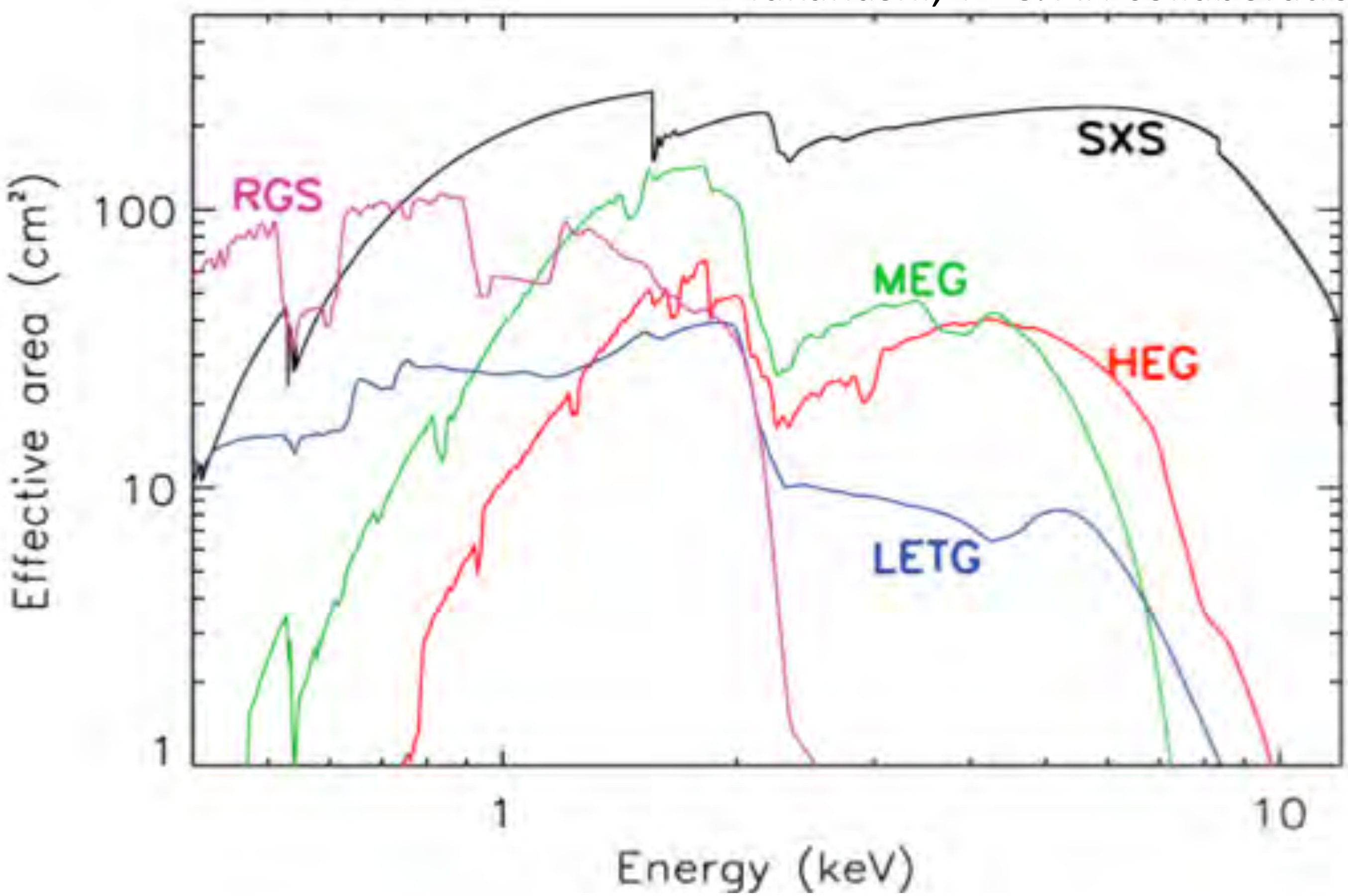

R. Petre

The SXS simulation (1) The Perseus center

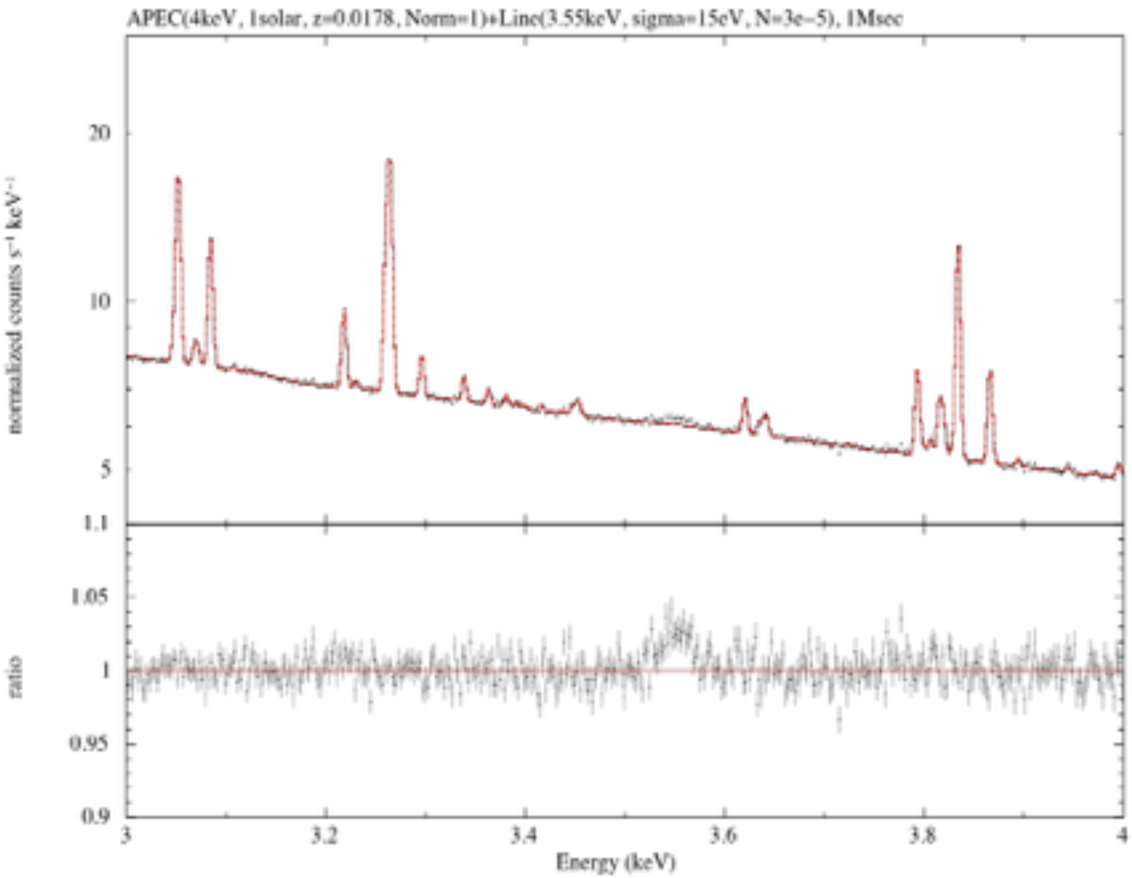

A simulation of 1Msec observation with a dark matter line at 3.55keV. We assume a ICM thermal emission of kT=4keV, 0.7solar, z=0.0178, and a X-ray flux of the Perseus center. No turbulent line broadening is assumed. For the dark matter emission, line broadening of a FWHM of 35eV by σ=1300km/velocity dispersion is assumed. Line flux is 3×10^{-5} ph/s/cm^2 (Bulbul+2014).The model in red assumes no DM line.

Provided by T. Tamura